# The Role of Amyloid PET in Imaging Neurodegenerative Disorders: A Review

Marianne Chapleau[1], Leonardo Iaccarino[1], David Soleimani-Meigooni[1], and Gil D. Rabinovici[1–3]

*[1]Memory and Aging Center, Department of Neurology, University of California, San Francisco, San Francisco, California; [2]Weill Institute for Neurosciences, University of California, San Francisco, San Francisco, California; and [3]Department of Radiology and Biomedical Imaging, University of California, San Francisco, San Francisco, California*

Imaging of amyloid deposition using PET has been available in research studies for 2 decades and has been approved for clinical use by the U.S. Food and Drug Administration, the European Medicines Agency, and other regulatory agencies around the world. Amyloid PET is a crucial tool for the diagnosis of Alzheimer disease, as it allows the noninvasive detection of amyloid plaques, a core neuropathologic feature that defines the disease. The clinical use of amyloid PET is expected to increase with recent accelerated approval in the United States of aducanumab, an antiamyloid monoclonal antibody, for the treatment of mild cognitive impairment and mild dementia due to Alzheimer disease. However, amyloid pathology can also be found in cognitively unimpaired older adults and in patients with other neurodegenerative disorders. The aim of this review is to provide an up-to-date overview of the application of amyloid PET in neurodegenerative diseases. We provide an in-depth analysis of the clinical, pathologic, and imaging correlates; a comparison with other available biomarkers; and a review of the application of amyloid PET in clinical trials and clinical utility studies.

**Key Words:** neurology; PET; PET/MRI; Alzheimer disease; amyloid PET; neurodegenerative diseases

**J Nucl Med 2022; 63:13S–19S**
DOI: 10.2967/jnumed.121.263195

Alzheimer disease (AD) is defined by the pathologic accumulation of amyloid-β (Aβ) plaques and tau neurofibrillary tangles (*1*). The accumulation of plaques (and to a lesser extent tangles) begins 10–20 y before the onset of clinical impairment (*2*). Aβ polypeptides are formed by cleavage of the amyloid precursor protein into 38–43 amino acid polypeptide fragments. The 40–42 amino acid Aβ polypeptides tend to form soluble aggregates (also known as Aβ oligomers) that further aggregate into microscopically detectable extracellular diffuse deposits (diffuse plaques, composed primarily of $A\beta_{42}$) and finally more dense neuritic plaques (Fig. 1A), which also contain tau-positive neurites. $A\beta_{40}$ polypeptides aggregate in blood vessel walls to form cerebral amyloid angiopathy (CAA) (Fig. 1B). At autopsy, amyloid accumulation is staged using the Thal phase and CERAD score (Consortium to Establish a Registry for Alzheimer's Disease). Thal phase describes the topography of Aβ plaques (diffuse or neuritic) in 5 phases, beginning in the association neocortex and spreading progressively through the paralimbic and limbic cortex, diencephalon, brain stem, and cerebellum (Fig. 1C). The CERAD score is based on the maximal density of neuritic plaques observed in one or more standardly sampled brain regions (categorized as sparse, moderate, or frequent; Fig. 1D). The overall degree of AD neuropathologic change is determined by integrating Thal phase, CERAD score, and Braak stage, the latter being a measure of the spread of intraneuronal neurofibrillary tangles.

The abnormal accumulation of both amyloid and tau can be quantified in vivo using PET imaging (*3,4*). In 2004, Klunk et al. reported the first successful attempt to image amyloid plaques in AD, applying the radiotracer $^{11}$C-labeled Pittsburgh compound B ($^{11}$C-PiB) (*5*). $^{11}$C-PiB was developed as an analog of thioflavin-T, a dye used by pathologists to stain amyloid in brain tissue. At the nanomolar concentrations injected for human imaging, $^{11}$C-PiB binds with high sensitivity and specificity to fibrillar Aβ aggregates (neuritic more than diffuse plaques), as well as to vascular amyloid in CAA. A major limitation of $^{11}$C-PiB is the 20-min half-life of the $^{11}$C radioisotope, limiting the use of this tracer to research PET centers equipped with a cyclotron. Since the advent of $^{11}$C-PiB, several tracers labeled with $^{18}$F (110-min half-life) have been developed that can be distributed from commercial cyclotrons for more widespread applications. These include $^{18}$F-florbetapir (Amyvid; Eli Lilly and Company), $^{18}$F-florbetaben (Neuraceq; Life Molecular Imaging), $^{18}$F-flutemetamol (Vizamyl; GE Healthcare), and $^{18}$F-flutafuranol (also known as NAV4694) (*6*). $^{11}$C-PiB and $^{18}$F-flutemetamol belong to the chemical class of benzothiazoles, whereas $^{18}$F-florbetaben and $^{18}$F-florbetapir are derived from stilbene and $^{18}$F-flutafuranol from benzofuran (Fig. 2). These compounds, although different in their chemical composition, all share a high affinity for fibrillar amyloid aggregates (*7*), allowing the detection of amyloid pathology in AD (*8*) and other diseases that involve fibrillar Aβ deposition (*9*).

In 2018, a National Institute on Aging and Alzheimer's Association (NIA-AA) research framework was proposed to standardize the evaluation of AD with biomarkers in living individuals (*10*). Biomarkers were grouped into those that measure amyloid deposition (cerebrospinal fluid [CSF] or PET), pathologic tau (CSF or PET), and neurodegeneration (CSF, PET, or MRI). In this research framework, the definition of AD is based purely on biomarker abnormalities (irrespective of clinical symptoms or stage), with AD defined as abnormal amyloid and tau biomarkers (A-positive, T-positive) whereas the Alzheimer continuum is defined as amyloid without tau (A-positive, T-negative). Although the NIA-AA research framework was intended for use only in the research setting, the 2021 International Working Group recommendations describe how AD biomarkers can be used to

Received Jan. 24, 2022; revision accepted Mar. 22, 2022.
For correspondence or reprints, contact Marianne Chapleau (marianne.chapleau@ucsf.edu).

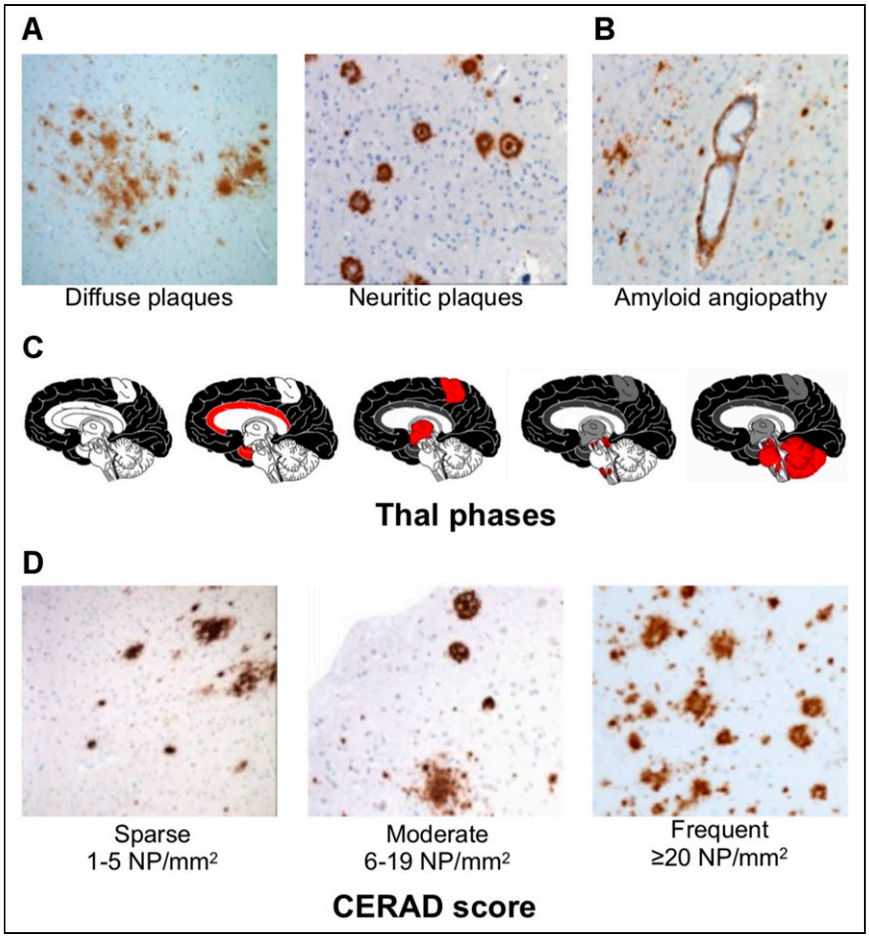


**FIGURE 1.** Postmortem measures of amyloid pathology. (A) Types of amyloid deposits. (B) Amyloid angiopathy. (C) Distribution of diffuse and neuritic plaques. (D) Neuritic plaque density (highest density score observed in brain). (A, B, and D are from UCSF Neurodegenerative Disease Brain Bank; C is reprinted with permission of (*53*).) NP = neuritic plaques.

supplement a clinical evaluation and support a diagnosis of AD in the clinic (*11*). In both contexts, assessing the utility of amyloid PET for diagnostic purposes is crucial, as in vivo biomarkers are increasingly playing a major role in research studies and the clinic. Furthermore, biomarkers such as amyloid PET will increasingly be used to assess the eligibility of patients for emerging anti-Aβ therapeutics such as aducanumab, an anti-Aβ monoclonal antibody recently granted accelerated approval in the United States for the treatment of mild cognitive impairment (MCI) or mild dementia due to AD (*12*). The aim of this review is to provide an overview of the application of amyloid PET in neurodegenerative diseases.

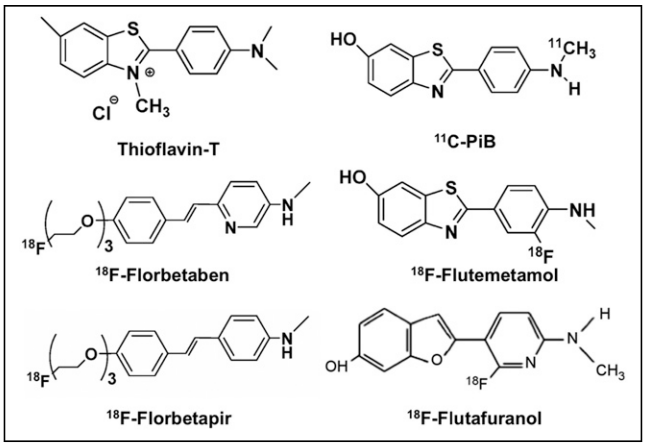


**FIGURE 2.** Structures of thioflavin-T, $^{11}$C-PiB, $^{18}$F-flutafuranol, and Food and Drug Administration–approved Aβ PET tracers. (Reprinted from (*54*).)

## VISUAL INTERPRETATION, QUANTIFICATION, AND THRESHOLDS

The typical distribution of amyloid PET uptake includes large portions of the neocortex and striatum, with relative sparing of the medial temporal lobes and primary unimodal cortices. This topography is consistent with the known postmortem distribution of amyloid pathology. The earliest and peak tracer uptake is usually observed in the posterior cingulate/precuneus and medial prefrontal regions (*13*). All Aβ tracers show nonspecific retention in the white matter, regardless of the presence of amyloid pathology. Tracer retention is more strongly linked to neuritic than diffuse plaques (*14*). Patients with CAA can present with occipital lobe–predominant retention (a common region in which CAA develops) (*15*), but the utility of amyloid PET for distinguishing between different types of Aβ deposits at the individual subject level is limited. Importantly, amyloid PET ligands do not bind to soluble Aβ oligomers, which have the highest neurotoxicity across Aβ aggregates.

Amyloid PET can be interpreted as positive or negative (or, alternatively, as elevated amyloid or nonelevated amyloid) on the basis of visual reads (Fig. 3; Table 1). In a negative scan, binding is restricted to white matter, showing a preserved gray matter–to–white matter contrast. Conversely, in a positive scan, cortical gray matter binding is equal to or greater than binding in the white matter, with subsequent loss of gray matter–to–white matter contrast. Despite slight differences in guidelines for visual interpretations among the clinically available amyloid PET tracers (Table 1), these positive and negative patterns tend to be consistent overall.

Cortical retention can also be quantified as a continuous measure, using a variety of PET modeling methods. The most common method involves calculation of tissue ratios between the target tissues (typically large regions of cortical gray matter) and a reference region known to be relatively devoid of amyloid until advanced stages (various combinations of cerebellum gray and white matter and brain stem), resulting in SUV ratios. The SUV ratio method is pragmatic in that reliable semiquantification can be accomplished with 10- to 20-min scans, but the method also has limitations compared with more rigorous quantification methods, including overestimation of the true concentration of pathology, and susceptibility to changes in blood flow. The centiloid method, which is derived from SUV ratio measurements, generates standardized units that can facilitate comparisons between tracers

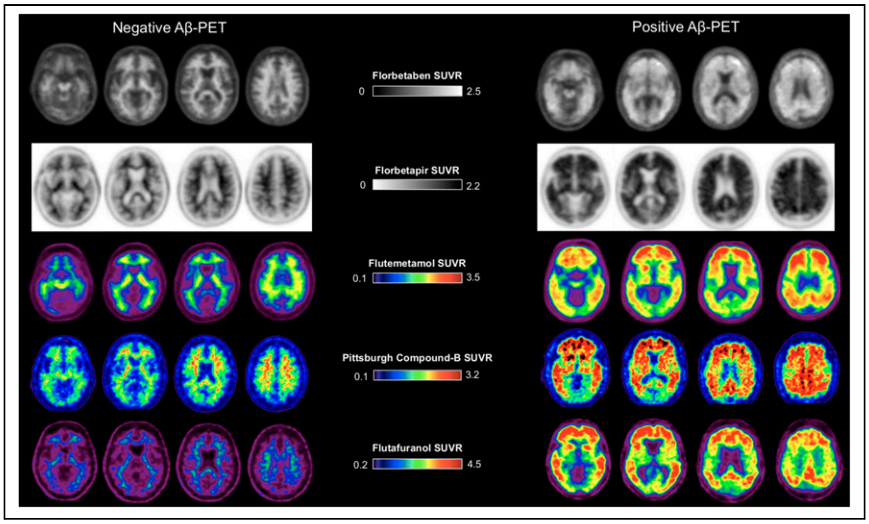


**FIGURE 3.** Examples of negative and positive Aβ PET findings using different tracers. ($^{18}$F-flutafuranol images are courtesy of Victor Villemagne and Christopher C. Rowe.)

and image processing methods. On this scale, 0 centiloid represents mean uptake in young adults devoid of amyloid, 12–25 centiloid represents a threshold for scan positivity, and 100 centiloid corresponds to the mean uptake in patients with mild AD dementia (*16,17*). Visual interpretations of amyloid PET are currently the standard in clinical practice, whereas SUV ratio and centiloid measurements are often used in research studies and drug trials.

The validation of amyloid PET as a reliable proxy for amyloid accumulation is based on PET-to-autopsy studies, in which individuals were imaged during life, and results were compared with the distribution and burden of amyloid after death (*17*). Visual reads of scans with $^{18}$F-labeled tracers as positive or negative, performed knowledge of any clinical information, showed 88%–98% sensitivity and 80%–95% specificity in distinguishing older adults with moderate to frequent neuritic plaques (according to the CERAD scale) from those with absent to sparse plaques (*18–20*). Quantification of $^{11}$C-PiB scans in patients with postmortem assessments show similar accuracy and reliably distinguish patients in Thal phases 3–5 from those in phases 0–2 (*17*). On the basis of these data, $^{18}$F-florbetapir, $^{18}$F-florbetaben, and $^{18}$F-flutemetamol were approved for clinical use by the U.S. Food and Drug Administration, the European Medicines Agency, and other regulatory agencies around the world.

## CLINICOIMAGING CORRELATES

Many studies have evaluated the prevalence of amyloid PET positivity in different clinical populations. In cognitively unimpaired older adults, amyloid PET scans are negative in 70%–90%, depending on age and apolipoprotein E (*APOE*) genotype (*21*). However, a considerable percentage of cognitively unimpaired older (>70 y old) subjects carry a significant amyloid burden (*21,22*), heightening the risk of false-positive findings (i.e., positive amyloid PET findings unrelated to the patient's symptoms) in older individuals. The prevalence of amyloid PET positivity in cognitively unimpaired adults increases linearly with age (~10% at age 50 y, ~15% at age 60 y, ~20% at age 70 y, ~30% at age 80 y, and ~40% at age 90 y). Additionally, the likelihood of amyloid positivity is strongly linked to *APOE* genotype, with people carrying at least 1 *APOE ε4* allele (the strongest genetic risk factor for sporadic AD) having a 2–3 times higher prevalence of amyloid pathology in any given age group (*21*).

As a group, cognitively unimpaired older adults who are amyloid PET–positive are at increased risk for developing MCI or dementia in subsequent years (*23*), though lifetime risk for any individual may be relatively low (*24*). The NIA-AA research framework considers cognitively unimpaired individuals to have preclinical AD if both amyloid and tau PET or CSF biomarkers are positive and to be on the AD continuum if their biomarker profile is A-positive, T-negative (*10*). The International Working Group recommendations take a slightly different approach, stratifying asymptomatic people into different risk levels depending on their genetic and biomarker profile (*11*).

The prevalence of amyloid PET positivity in patients with MCI is 27%–71% depending on the specific criteria used, increasing also with age and *APOE ε4* genotype (*21*). Amyloid PET is useful in identifying when MCI is due to underlying AD pathology and is included in the research diagnostic criteria for MCI due to AD (*25*) or prodromal AD (*11*) (Fig. 4). Amyloid PET positivity is associated with a 3–4 times increased risk of conversion to AD dementia over the next 3–5 y after adjusting for age, APOE genotype, and other covariates. However, the individual trajectories of amyloid-positive MCI patients are highly variable at the single-patient level (*26*). The combination of amyloid PET positivity, APOE4 genotype, and positive biomarkers of tau (CSF or PET) or neurodegeneration (MRI or $^{18}$F-FDG PET) increases the risk of conversion in the shorter term (*27–29*).

Approximately 70%–90% of patients meeting the clinical criteria for dementia due to AD have positive amyloid PET results (*30,31*). Interestingly, the prevalence of amyloid positivity decreases with age in patients clinically diagnosed with probable AD, probably because of an increase in the prevalence of non-Aβ brain pathologies that present with an amnestic dementia in older patients (e.g., limbic system–associated TDP-43 encephalopathy, vascular contributions to impairment and dementia, and primary age-related tauopathy) (*31*). The prevalence of amyloid pathology in cognitively unimpaired older adults is an important consideration in interpreting the clinical meaning of an amyloid PET scan. Although a negative amyloid PET result is useful for excluding AD at any age, the positive predictive value of amyloid PET decreases with increasing age, since at an older age it is more likely that the finding of amyloid is incidental, and the patient may have another condition that is primarily responsible for the symptoms. At the dementia stage, amyloid PET is useful for distinguishing AD from neurodegenerative conditions that are not associated with Aβ, such as frontotemporal dementia (*32,33*). Since amyloid and tau burden are positively correlated, a positive amyloid PET result is often associated with significant tau pathology and intermediate to high overall AD neuropathology (*33*), and amyloid PET has higher sensitivity than $^{18}$F-FDG PET for detecting clinically meaningful AD neuropathology. Amyloid PET is not useful at distinguishing AD from other disorders that involve Aβ deposits, such as dementia with Lewy bodies (50%–70% amyloid PET–positive) and CAA.

**TABLE 1**
Summary Guidelines for Interpretation of Amyloid PET Scans Using Different Tracers

| Tracer category | Tracer name | Dose and acquisition protocol (clinical) | Visualization | Interpretation criteria for positive scan |
|---|---|---|---|---|
| Food and Drug Administration–approved | $^{18}$F-florbetaben | ~300 MBq; 15- to 20-min acquisition beginning at 45–130 min (research use, 20-min acquisition beginning at 90–110 min) | Gray scale; window images to optimize GM/WM contrast in cerebellum | Increased GM uptake extending to cortical margin involving most slices in at least 1 of 4 target cortical regions: frontal, parietal, precuneus/posterior cingulate, lateral temporal; regional cortical tracer uptake/brain amyloid plaque load scores (*20*) |
| | $^{18}$F-florbetapir | ~370 MBq; 10- to 20-min acquisition beginning at 30–50 min (package insert guidelines) for clinical use or 50–70 min (optimized kinetics for quantification) for research use | Inverse gray scale; window images to optimize GM/WM contrast in cerebellum | Loss of GM/WM contrast due to increased cortical binding in, first, 2 or more brain areas (each larger than single gyrus) with reduced or absent GM/WM contrast or, second, 1 or more areas with intense signal where GM > WM |
| | $^{18}$F-flutemetamol | ~185 MBq; 10- to 20-min acquisition at 60–120 min (research use, 20-min acquisition at 90–110 min) | Color scale (NIH); normalize so that pons is at 90% of activity | Increased GM uptake (>50%–60% peak intensity) or loss of GM matter contrast in at least 1 of 4 cortical regions and 1 subcortical region: frontal, inferolateral parietal, precuneus/posterior cingulate, lateral temporal, striatum |
| Research | $^{11}$C-PiB | ~555 MBq; dynamic 60- to 90-min acquisition (distribution volume ratio) or 20-min acquisition at 50–70 min (SUV ratio) | Color scale (NIH); window images to optimize GM/WM contrast in cerebellum | No formal guidelines for reading (research use only) |
| | $^{18}$F-flutafuranol | ~185 MBq; 20- to 30-min acquisition beginning at 40–50 min | Color scale (NIH); window images to optimize GM/WM contrast in cerebellum | No formal guidelines for reading (research use only) |

GM = gray matter; NIH = National Institutes of Health; WM = white matter.

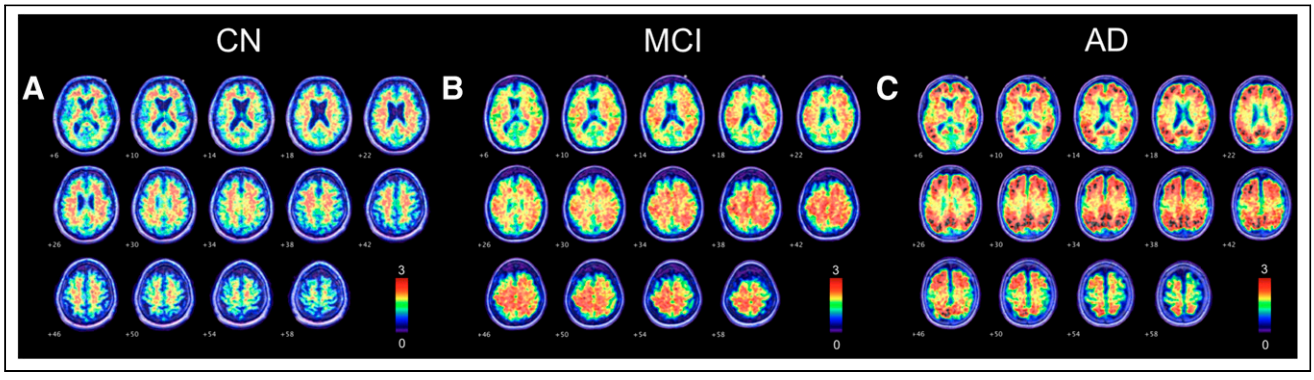


**FIGURE 4.** Evolution of amyloid PET positivity across AD spectrum. (A) Positive $^{11}$C-PiB scan of cognitively normal (CN) participant, in which significant binding is observed in precuneus, posterior cingulate cortex, and medial prefrontal areas. (B) Positive $^{11}$C-PiB scan of MCI patient, in which significant and moderate binding is observed throughout cortex. (C) Positive $^{11}$C-PiB scan of AD patient, in which significant and severe binding is observed throughout cortex.

## APPROPRIATE-USE CRITERIA (AUCS)

AUCs published in 2013 highlight appropriate and inappropriate clinical uses of amyloid PET. The AUCs state that clinical amyloid PET may be considered in patients with objectively confirmed cognitive impairment (i.e., MCI or dementia) but in whom the cause of impairment is uncertain after a comprehensive evaluation by a dementia specialist (including CT/MRI) and for whom knowledge of amyloid PET results is expected to increase diagnostic certainty and change patient management. The patients most likely to benefit include those with persistent or progressive unexplained MCI, those with possible AD but an atypical course or etiologically mixed presentation, and those with young-onset dementia (before age 65 y). Inappropriate scenarios include use for assessing dementia severity, use in unimpaired individuals (with or without subjective complaints), and nonmedical uses (e.g., legal, insurance coverage, or employment screening). An update to the AUCs is expected in 2022, incorporating tau PET and addressing the emerging availability of approved anti-Aβ therapeutics.

## CLINICAL UTILITY STUDIES

The clinical utility of amyloid PET has been reviewed (*34,35*) and assessed in various multisite cohort studies, including the Imaging Dementia–Evidence for Amyloid Scanning (IDEAS) study, the Amyloid Imaging to Prevent Alzheimer's Disease–Diagnostic and Patient Management Study (AMYPAD-DPMS) study, the Alzheimer Biomarkers in Daily Practice (ABIDE) study, and a randomized clinical trial (*36*). The IDEAS study was a United States–wide longitudinal study evaluating the impact of amyloid PET and health outcomes in over 18,000 patients with MCI or dementia who met the AUCs and were recruited at nearly 600 specialty clinics across the United States. The study was conducted in collaboration with the U.S. Centers for Medicare and Medicaid Services under Coverage with Evidence Development. Amyloid PET was associated with implemented changes in core elements of patient management 90 d after the scan in 60.2% of patients with MCI and 63.5% of patients with dementia, far exceeding the study's goal of a change in management in at least 30% of patients in each group. The most common change involved the use of approved medications (i.e., cholinesterase inhibitors or memantine) for AD (43.6% in MCI and 44.9% in dementia). The diagnosis changed after PET in about 35% of patients (25% switched from AD to non-AD, and 10% switched from non-AD to AD) (*30*). The impact of amyloid PET on health outcomes was more modest. Rates of 12-mo hospitalizations after PET were 23.98% in IDEAS participants, compared with 25.12% in a matched cohort of Medicare beneficiaries who had not undergone amyloid PET (4.5% relative reduction), falling short of the prespecified goal of no more than a 10% relative reduction (*37*). There was no significant difference in 12-mo rates of emergency department visits between IDEAS participants and controls. These results, in addition to the approval of novel amyloid-lowering treatments for AD, will inform future coverage policies for Centers for Medicare and Medicaid Services and other payers in the United States and globally.

The ABIDE project also assessed the association between amyloid PET and changes in diagnosis, diagnosis confidence, treatment, and patients' experiences in a memory clinic at the Vrije Universiteit Medical Center, The Netherlands (*38*). The authors found that the etiologic diagnosis changed for 25% of patients after amyloid PET, more often because of a negative than a positive scan. Also, diagnostic confidence increased, and for some patients, there was a change in the treatment received. The European AMYPAD-DPMS study has a similar goal of determining the value of amyloid imaging as a diagnostic and therapeutic marker for AD to supply physicians and health-care payers with data to plan management decisions (*39*). Results regarding this multisite project are pending. Another multicenter, randomized, and controlled study (*36*) showed that knowledge of the amyloid status affects diagnosis and patient management and involves mainly changes in AD medications.

## COMPARISON WITH FLUID BIOMARKERS

Concentrations of monomeric Aβ, total tau, and phosphorylated tau (at various epitopes) can also be measured in CSF and plasma. The ratio of CSF $A\beta_{42/40}$ concentrations is highly congruent with amyloid PET in classifying individuals as amyloid-positive or -negative (*40*), as is the ratio of $A\beta_{42}$ with total or phosphorylated tau (*41*). Changes in Aβ are likely detectable earlier in CSF than by amyloid PET (*42*). Similarly, novel plasma assays that measure $A\beta_{42/40}$ in plasma using mass spectrometry or highly sensitive immunoassays show high concordance with amyloid PET and CSF (*43–45*). Plasma measurements of phosphorylated tau also show promise in detecting brain amyloidosis (*46–48*). Compared with CSF, plasma Aβ and tau biomarkers are in earlier stages of standardization and require additional validation before clinical use. A future diagnostic algorithm for amyloid pathology may begin with plasma measurements, followed by more definitive CSF or amyloid PET testing. CSF and PET can be used interchangeably in the clinic, though amyloid PET would be the first-line test in patients in whom CSF is contraindicated (e.g., patient who are anticoagulated) or would be considered in patients with equivocal CSF results (*49*).

## CLINICAL TRIALS

Over the past decade, amyloid PET has been used in clinical trials to screen for treatment eligibility (i.e., to provide evidence of amyloid pathology) and assess target engagement for drugs designed to reduce amyloid plaques, most notably anti-Aβ monoclonal antibodies. The accelerated approval of aducanumab, an anti-Aβ monoclonal antibody that targets Aβ fibrils, in June 2021 by the U.S. Food and Drug Administration was based on the drug's dose-dependent ability to reduce amyloid PET signal (*12*). Although the drug reduced amyloid PET signal in 2 identically designed phase 3 randomized controlled trials, a significant (though modest) slowing of clinical decline was observed in only one study. Food and Drug Administration approval was based on lowering of amyloid on PET as a surrogate biomarker reasonably likely to predict clinical benefit, but a confirmatory trial evaluating clinical benefit was required as part of the accelerated approval pathway. Amyloid PET has also been a key outcome measure in trials of the potent anti-Aβ monoclonals donanemab (*50*), lecanemab (*51*), and gantenerumab (*52*). In early-phase studies, all antibodies convincingly lowered amyloid PET, and donanemab and lecanemab showed early evidence supportive of modest clinical benefit as well. Phase 3 randomized controlled trials of these antibodies are expected in the coming 1–2 years. In the donanemab phase 2 study, amyloid PET was used not only to select patients but also to titrate treatment. Drug dose was lowered on the basis of the amyloid PET response, and the drug was ultimately

switched to placebo when the scan findings were negative. This could represent an important future clinical algorithm for determining the duration of treatment with this class of drugs.

## CONCLUSION

Amyloid PET can detect cerebral Aβ deposition with precision, has good specificity for AD neuropathology, can inform on the presence of contributing amyloid copathology in other diseases, and will inform eligibility for emerging anti-Aβ therapeutics. Amyloid PET is a reliable diagnostic imaging tool, and its use should be encouraged to guide early differential diagnosis in clinical settings and, in the future, to select patients for disease-specific therapies.

## DISCLOSURE

Marianne Chapleau received research support from the Fonds de recherche du Québec - Santé (FRQS). Gil Rabinovici receives research support from NIH/NIA R35 AG072362, NIH/NIA, and P30 AG062422; has served on Scientific Advisory Boards for Eisai, Eli Lilly, Genentech, and Roche; serves on a Data Safety and Monitoring Board for Johnson & Johnson; and is an associate editor for *JAMA Neurology*. Other support includes NINDS, AA, American College of Radiology, Rainwater Charitable Foundation, Shanendoah Foundation, Avid Radiopharmaceuticals, GE Healthcare, Life Molecular Imaging, and Genentech. No other potential conflict of interest relevant to this article was reported.

## REFERENCES


1. DeTure MA, Dickson DW. The neuropathological diagnosis of Alzheimer's disease. *Mol Neurodegener.* 2019;14:32.
2. Sperling RA, Aisen PS, Beckett LA, et al. Toward defining the preclinical stages of Alzheimer's disease: recommendations from the National Institute on Aging-Alzheimer's Association workgroups on diagnostic guidelines for Alzheimer's disease. *Alzheimers Dement.* 2011;7:280–292.
3. Schöll M, Lockhart SN, Schonhaut DR, et al. PET imaging of tau deposition in the aging human brain. *Neuron.* 2016;89:971–982.
4. Ossenkoppele R, Schonhaut DR, Scholl M, et al. Tau PET patterns mirror clinical and neuroanatomical variability in Alzheimer's disease. *Brain.* 2016;139:1551–1567.
5. Klunk WE, Engler H, Nordberg A, et al. Imaging brain amyloid in Alzheimer's disease with Pittsburgh compound-B. *Ann Neurol.* 2004;55:306–319.
6. Villemagne VL, Dore V, Burnham SC, Masters CL, Rowe CC. Imaging tau and amyloid-beta proteinopathies in Alzheimer disease and other conditions. *Nat Rev Neurol.* 2018;14:225–236.
7. Querfurth HW, LaFerla FM. Alzheimer's disease. *N Engl J Med.* 2010;362:329–344.
8. Dickerson BC, McGinnis SM, Xia C, et al. Approach to atypical Alzheimer's disease and case studies of the major subtypes. *CNS Spectr.* 2017;22:439–449.
9. Rostagno A, Holton JL, Lashley T, Revesz T, Ghiso J. Cerebral amyloidosis: amyloid subunits, mutants and phenotypes. *Cell Mol Life Sci.* 2010;67:581–600.
10. Jack CR Jr, Bennett DA, Blennow K, et al. NIA-AA research framework: toward a biological definition of Alzheimer's disease. *Alzheimers Dement.* 2018;14:535–562.
11. Dubois B, Villain N, Frisoni GB, et al. Clinical diagnosis of Alzheimer's disease: recommendations of the international working group. *Lancet Neurol.* 2021;20:484–496.
12. Rabinovici GD. Controversy and progress in Alzheimer's disease: FDA approval of aducanumab. *N Engl J Med.* 2021;385:771–774.
13. Villeneuve S, Rabinovici GD, Cohn-Sheehy BI, et al. Existing Pittsburgh compound-B positron emission tomography thresholds are too high: statistical and pathological evaluation. *Brain.* 2015;138:2020–2033.
14. Seo SW, Ayakta N, Grinberg LT, et al. Regional correlations between [$^{11}$C]PIB PET and post-mortem burden of amyloid-beta pathology in a diverse neuropathological cohort. *Neuroimage Clin.* 2016;13:130–137.
15. Johnson KA, Gregas M, Becker JA, et al. Imaging of amyloid burden and distribution in cerebral amyloid angiopathy. *Ann Neurol.* 2007;62:229–234.
16. Klunk WE, Koeppe RA, Price JC, et al. The centiloid project: standardizing quantitative amyloid plaque estimation by PET. *Alzheimers Dement.* 2015;11:1–15.e4.
17. La Joie R, Ayakta N, Seeley WW, et al. Multisite study of the relationships between antemortem [$^{11}$C]PIB-PET centiloid values and postmortem measures of Alzheimer's disease neuropathology. *Alzheimers Dement.* 2019;15:205–216.
18. Clark CM, Pontecorvo MJ, Beach TG, et al. Cerebral PET with florbetapir compared with neuropathology at autopsy for detection of neuritic amyloid-beta plaques: a prospective cohort study. *Lancet Neurol.* 2012;11:669–678.
19. Curtis C, Gamez JE, Singh U, et al. Phase 3 trial of flutemetamol labeled with radioactive fluorine 18 imaging and neuritic plaque density. *JAMA Neurol.* 2015;72:287–294.
20. Sabri O, Sabbagh MN, Seibyl J, et al. Florbetaben PET imaging to detect amyloid beta plaques in Alzheimer's disease: phase 3 study. *Alzheimers Dement.* 2015;11:964–974.
21. Jansen WJ, Ossenkoppele R, Knol DL, et al. Prevalence of cerebral amyloid pathology in persons without dementia: a meta-analysis. *JAMA.* 2015;313:1924–1938.
22. Jansen WJ, Janssen O, Tijms BM, et al. Prevalence estimates of amyloid abnormality across the Alzheimer disease clinical spectrum. *JAMA Neurol.* 2022;79:228–243.
23. Donohue MC, Sperling RA, Petersen R, et al. Association between elevated brain amyloid and subsequent cognitive decline among cognitively normal persons. *JAMA.* 2017;317:2305–2316.
24. Brookmeyer R, Abdalla N. Estimation of lifetime risks of Alzheimer's disease dementia using biomarkers for preclinical disease. *Alzheimers Dement.* 2018;14:981–988.
25. Albert MS, DeKosky ST, Dickson D, et al. The diagnosis of mild cognitive impairment due to Alzheimer's disease: recommendations from the National Institute on Aging-Alzheimer's Association workgroups on diagnostic guidelines for Alzheimer's disease. *Alzheimers Dement.* 2011;7:270–279.
26. Jutten RJ, Sikkes SAM, Amariglio RE, et al. Identifying sensitive measures of cognitive decline at different clinical stages of Alzheimer's disease. *J Int Neuropsychol Soc.* 2021;27:426–438.
27. Wolk DA, Sadowsky C, Safirstein B, et al. Use of flutemetamol F 18-labeled positron emission tomography and other biomarkers to assess risk of clinical progression in patients with amnestic mild cognitive impairment. *JAMA Neurol.* 2018;75:1114–1123.
28. Mormino EC, Betensky RA, Hedden T, et al. Amyloid and APOE epsilon4 interact to influence short-term decline in preclinical Alzheimer disease. *Neurology.* 2014;82:1760–1767.
29. van der Kall LM, Truong T, Burnham SC, et al. Association of beta-amyloid level, clinical progression, and longitudinal cognitive change in normal older individuals. *Neurology.* 2021;96:e662–e670.
30. Rabinovici GD, Gatsonis C, Apgar C, et al. Association of amyloid positron emission tomography with subsequent change in clinical management among Medicare beneficiaries with mild cognitive impairment or dementia. *JAMA.* 2019;321:1286–1294.
31. Ossenkoppele R, Jansen WJ, Rabinovici GD, et al. Prevalence of amyloid PET positivity in dementia syndromes: a meta-analysis. *JAMA.* 2015;313:1939–1949.
32. Rabinovici GD, Rosen HJ, Alkalay A, et al. Amyloid vs FDG-PET in the differential diagnosis of AD and FTLD. *Neurology.* 2011;77:2034–2042.
33. Lesman-Segev OH, La Joie R, Iaccarino L, et al. Diagnostic accuracy of amyloid versus $^{18}$F-fluorodeoxyglucose positron emission tomography in autopsy-confirmed dementia. *Ann Neurol.* 2021;89:389–401.
34. Barthel H, Sabri O. Clinical use and utility of amyloid imaging. *J Nucl Med.* 2017;58:1711–1717.
35. Cotta Ramusino M, Perini G, Altomare D, et al. Outcomes of clinical utility in amyloid-PET studies: state of art and future perspectives. *Eur J Nucl Med Mol Imaging.* 2021;48:2157–2168.
36. Pontecorvo MJ, Siderowf A, Dubois B, et al. Effectiveness of florbetapir PET imaging in changing patient management. *Dement Geriatr Cogn Disord.* 2017;44:129–143.
37. Rabinovici G, Iaccarino L, La Joie R, et al. Amyloid and tau PET in sporadic early-onset Alzheimer's disease: preliminary results from LEADS: LEADS: sporadic early-onset Alzheimer's disease in the spotlight. *Alzheimers Dement.* 2020;16:1–4.
38. de Wilde A, van der Flier WM, Pelkmans W, et al. Association of amyloid positron emission tomography with changes in diagnosis and patient treatment in an unselected memory clinic cohort: the ABIDE project. *JAMA Neurol.* 2018;75:1062–1070.
39. Frisoni GB, Barkhof F, Altomare D, et al. AMYPAD diagnostic and patient management study: rationale and design. *Alzheimers Dement.* 2019;15:388–399.
40. Hansson O, Lehmann S, Otto M, Zetterberg H, Lewczuk P. Advantages and disadvantages of the use of the CSF amyloid beta (Abeta) 42/40 ratio in the diagnosis of Alzheimer's disease. *Alzheimers Res Ther.* 2019;11:34.
41. Campbell MR, Ashrafzadeh-Kian S, Petersen RC, et al. P-tau/Abeta42 and Abeta42/40 ratios in CSF are equally predictive of amyloid PET status. *Alzheimers Dement (Amst).* 2021;13:e12190.

42. Palmqvist S, Mattsson N, Hansson O; Alzheimer's Disease Neuroimaging Initiative. Cerebrospinal fluid analysis detects cerebral amyloid-beta accumulation earlier than positron emission tomography. *Brain.* 2016;139:1226–1236.
43. Schindler SE, Bollinger JG, Ovod V, et al. High-precision plasma beta-amyloid 42/40 predicts current and future brain amyloidosis. *Neurology.* 2019;93: e1647–e1659.
44. Jang H, Kim JS, Lee HJ, et al. Performance of the plasma Abeta42/Abeta40 ratio, measured with a novel HPLC-MS/MS method, as a biomarker of amyloid PET status in a DPUK-KOREAN cohort. *Alzheimers Res Ther.* 2021;13:179.
45. Pérez-Grijalba V, Romero J, Pesini P, et al. Plasma Abeta42/40 ratio detects early stages of Alzheimer's disease and correlates with CSF and neuroimaging biomarkers in the AB255 study. *J Prev Alzheimers Dis.* 2019;6:34–41.
46. Thijssen EH, La Joie R, Strom A, et al. Plasma phosphorylated tau 217 and phosphorylated tau 181 as biomarkers in Alzheimer's disease and frontotemporal lobar degeneration: a retrospective diagnostic performance study. *Lancet Neurol.* 2021; 20:739–752.
47. Thijssen EH, La Joie R, Wolf A, et al. Diagnostic value of plasma phosphorylated tau181 in Alzheimer's disease and frontotemporal lobar degeneration. *Nat Med.* 2020;26:387–397.
48. Ashton NJ, Pascoal TA, Karikari TK, et al. Plasma p-tau231: a new biomarker for incipient Alzheimer's disease pathology. *Acta Neuropathol (Berl).* 2021; 141:709–724.
49. Engelborghs S, Niemantsverdriet E, Struyfs H, et al. Consensus guidelines for lumbar puncture in patients with neurological diseases. *Alzheimers Dement (Amst).* 2017;8:111–126.
50. Mintun MA, Lo AC, Duggan Evans C, et al. Donanemab in early Alzheimer's disease. *N Engl J Med.* 2021;384:1691–1704.
51. Swanson CJ, Zhang Y, Dhadda S, et al. A randomized, double-blind, phase 2b proof-of-concept clinical trial in early Alzheimer's disease with lecanemab, an anti-Abeta protofibril antibody. *Alzheimers Res Ther.* 2021;13:80.
52. Salloway S, Farlow M, McDade E, et al. A trial of gantenerumab or solanezumab in dominantly inherited Alzheimer's disease. *Nat Med.* 2021;27:1187–1196.
53. Thal DR, Rub U, Orantes M, Braak H. Phases of A beta-deposition in the human brain and its relevance for the development of AD. *Neurology.* 2002; 58:1791–1800.
54. Uzuegbunam BC, Librizzi D, Hooshyar Yousefi B. PET radiopharmaceuticals for Alzheimer's disease and Parkinson's disease diagnosis, the current and future landscape. *Molecules.* 2020;25:977.